DOI: 10.48011/asba.v2i1.1182

Transient Voltages on Grounding Grids buried in Stratified Soils

Anderson R. J. de Araújo * **Walter L. M. de Azevedo** *
José Pissolato Filho * **Jaimis S. L. Colqui** **
Sérgio Kurokawa **

* *School of Electrical and Computer Engineering, University of Campinas, Campinas, SP, Brazil (e-mails:ajusto@dsce.fee.unicamp.br, w157573@dac.unicamp.br, pisso@dsce.fee.unicamp.br)*
** *Dep. of Electrical Engineering-São Paulo State University, Ilha Solteira, SP, Brazil (e-mails: jaimis.leon@unesp.br, sergio.kurokawa@unesp.br)*

Abstract: Grounding grids (GG) play a fundamental role in the protection of personnel and prevention of damages in equipment during surge transients on substations caused by lightning discharges on power systems. In this context, a precise GG modeling must consider several factors such as the arrangement and the soil compacted in stratified layers. This paper proposes a lumped approach for GG buried in several stratified soils to compute the transient node voltages when subjected to lightning strikes. The vertical and horizontal electrodes are modelled separately by lumped circuit approach. The vertical electrode impedances buried in a stratified soil are computed by the numerical Method of Moments (MoM) in the full-wave electromagnetic software FEKO®, directly in frequency domain, and then, an electric circuit is obtained by the Vector Fitting technique. The horizontal electrodes are modelled based on the electromagnetic radiation theory, where each segment of the electrode can be regarded as a filamental current-carrying conductor. Lightning currents of fast and slow-front waveforms, are employed in the simulations. Results show that when stratified soils are considered, the differences of the transient voltage peaks, in comparison with the ones calculated for the homogeneous soil is more pronounced as the thickness of soil decreases.

Resumo: Malhas de aterramento (MA) são essenciais na proteção de pessoas e na prevenção de danos aos equipamentos durante os transitórios causados por descargas atmosféricas nos sistemas elétricos. Um modelo preciso da MA deve considerar diversos fatores, tais como o arranjo da malha e as propriedades do solo estratificado. Este artigo propõe uma modelagem a parâmetros concentrados dos condutores para a representação de MA em solos estratificados e o cálculo das tensões transitórias nodais geradas por descargas atmosféricas injetadas. Os eletrodos verticais e horizontais são modelados separadamente. A impedância do eletrodo vertical é calculada pelo Método dos Momentos (MoM) no software FEKO®, diretamente no domínio de frequência, e um circuito equivalente é proposto usando a técnica do Vector Fitting. Os eletrodos horizontais são modelados com base na teoria eletromagnética, onde cada segmento conduz uma corrente filamentar. Descargas atmosféricas, do tipo frente rápida e lenta, são empregadas nas simulações. Os resultados mostram que quando o solo é estratificado a diferença entre os picos das tensão transitórias, em comparação com aqueles obtidos para um solo homogêneo, é mais pronunciada conforme a espessura da primeira camada de solo diminui.

Keywords: Electromagnetic transients; grounding electrodes; grounding impedance; stratified soils.

Palavras-chaves: transitórios eletromagnéticos; eletrodos de aterramento; impedância de aterramento; solos estratificados.

1. INTRODUCTION

A well-design grounding grid must provide a low-path impedance into ground to dissipate effectively the high currents caused by either faults or lightning strikes on electrical power systems. Furthermore, grounding grids are designed to minimize the ground potential rise (GPR) to protect any person in the vicinity, safeguard equipment inside electrical substations and to ensure a reliable operation during the transient period (Gouda et al., 2019; Ghania, 2019).

In this context, several approaches to model the grounding grids and to computed its grounding impedances are proposed in the literature. They can be based on analytical formulae, lumped or distributed circuit representation and full-wave electromagnetic modeling (EM) combining numerical methods such as: Method of Moments (MoM) (Ghomi et al., 2019), Finite Element Method (FEM) (Liu et al., 2005), Finite-Difference Time-Domain (FDTD) (Baba et al., 2005) method and Partial Electric Equivalent Circuit (PEEC) (Sarajcev e Vujevic, 2009; Salarieh et al., 2020). The EMs are the most rigorous and accurate approaches, specially at high frequencies, however a high computational cost (memory storage) and time may be required for complex grounding systems due to the small discretization (meshing size) domain (Sekki et al., 2014; Chiheb et al., 2018).

Grounding grids consist of a large mesh of horizontal electrodes (HE) combined with long vertical electrodes (VE) which occupies a considerable area in the substation (Colominas et al., 2002). Many factors must be taken into account to accurately compute the grounding impedances of the grounding grids, such as: the inhomogeneity of soils (stratified layers of ground), frequency-dependence on the electrical soil parameters, mutual couplings, ionisation effects and grid arrangements (Yang et al., 2013; Kherif et al., 2017).

Many authors have dealt with the problem of calculating the apparent soil resistivity of stratified soils where different experimental set-ups and suggested formulae are proposed (Gouda et al., 2019; Batista e Paulino, 2019). In these equations, it is necessary to know the exact number of layers, electrode arrangement, the thickness of each layer and the reflection factor (k), further detailed (Gouda et al., 2019).

This paper proposes a lumped approach to represent grounding grids buried in a 2-layer soil and to compute the transient voltages on the mesh when it is subjected to two types of lightning strikes. The impedance of the vertical electrodes are computed by numerical numerical MoM in the full-wave electromagnetic software FEKO in full-wave electromagnetic software FEKO and then an equivalent circuit is fitted by the Vector Fitting technique. The horizontal electrodes are modelled by lumped circuit approach, based on the electromagnetic radiation theory, where each segment of the conductor can be regarded as a current-carrying conductor. Results show a significant reduction on the node transient voltages of the grid when a second layer of soil, with a lower resistivity than the previously homogeneous soil, is taken into account. In addition as the thickness of the soil layer with the lowest resistivity increases, the node transient voltages decreases. As advantages, the lumped representation is a friendly tool to compute the grounding impedances of cylindrical electrodes and grounding grids, and also the transient voltages on grids buried in stratified soils combined with low computational time.

⋆ This study received Financial support from São Paulo Research Foundation (FAPESP) (Grant: 2019/01396-1) and the Management Center of Technology and Innovation (CGTI).

2. LUMPED APPROACH FOR VERTICAL ELECTRODES IN A STRATIFIED SOIL

A vertical electrode buried in a homogeneous soil can be modeled by the its distributed parameters using the Transmission Line Model (TLM). In TLM, the same equations employed to compute voltages and currents along the line can be applied in the vertical electrode in order to obtain its grounding impedances. In Fig. 1a, a vertical rod of length L_v and radius r is buried in a two-layer soil characterized by the electrical parameters: ρ_i, ε_{ri} and μ_i being the resistivity, the relative permittivity and the relative permeability for each layer of soil, respectively (i = 1,2). Considering TLM, each electrode segment in the i-layer is represented by per-unit-length (p.u.l.) resistance r'_i, inductance L'_i, conductance G'_i and capacitance C'_i defined by (Grcev e Popov, 2005):

$$r'_i = \frac{R_i}{l^*} = \frac{\rho_c}{\pi r^2}; \tag{1a}$$

$$L'_i = \frac{L_i}{l^*} = \frac{\mu_r}{2\pi}\left[ln\left(\frac{2l^*}{r}\right) - 1\right]; \tag{1b}$$

$$G'_i = \frac{G_i}{l^*} = \frac{2\pi}{\rho_i}\left[ln\left(\frac{4l^*}{r}\right) - 1\right]^{-1}; \tag{1c}$$

$$C'_i = \frac{C_i}{l^*} = 2\pi\varepsilon_r\left[ln\left(\frac{4l^*}{r}\right) - 1\right]; \tag{1d}$$

where ρ_c is the conductor resistivity, l^* is the electrode length in each layer (i.e. $l^* = h$ for $i = 1$ and $l^* = L_v - h$ for $i = 2$) and $\mu_r \approx \mu_0$. The equivalent resistivity can be calculated by the Blattner's formula, given by (Caetano et al., 2018):

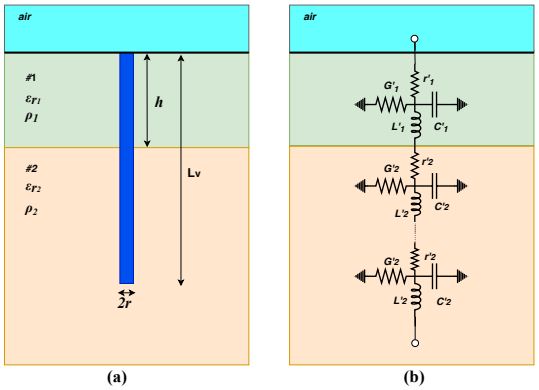

Fig. 1. Vertical rod buried in a two-layer soil: [(a) Generic representation and (b) distributed parameter representation of the electrode.]

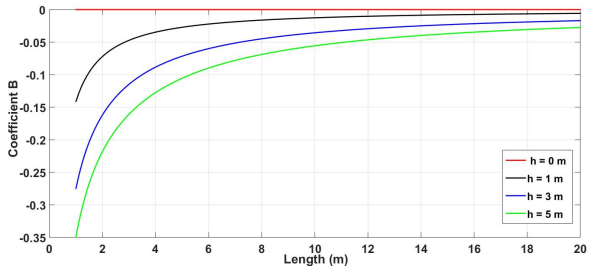

Fig. 2. Coefficient B as a function of electrode length (L_v) and first layer thickness (h).

$$\rho_{eq} = \frac{L_v \rho_1 \rho_2}{\rho_2 h + \rho_1 (L_v - h)} (1 + B), \tag{2a}$$

$$B = [ln(4L_v/r) - 1]^{-1} \sum_{n=1}^{\infty} k^n ln \left[\frac{2nh + L_v}{(2n-2)h + L_v} \right], \tag{2b}$$

$$k = \frac{\rho_2 - \rho_1}{\rho_2 + \rho_1} \tag{2c}$$

where k is called reflection factor and B is a correction factor. The influence on the correction factor B, considering ρ_1 = 1,000 Ωm and ρ_2 = 100 Ωm (k = -0.81) for some values of h is depicted in Fig.2.

Once the grounding impedances $Z_{eq}(s)$ are computed by the numerical MoM in the full-wave electromagnetic software FEKO ®, the frequency-dependent responses are approximated by accurate rational functions with stable-poles. This procedure can be done by the Vector Fitting (VF) technique (Gustavsen e Semlyen, 1999). The VF is a well-know tool used to fit the frequency-dependent curve into an equivalent electric circuit. The grounding admittance $Y_{eq}(s)$ ($Y_{eq}(s) = Z_{eq}^{-1}(s)$) can be written as a sum of rational functions as given by (Gustavsen e Semlyen, 1999; Vanegas et al., 2008):

$$Y_{eq}(s) \simeq \sum_{j=1}^{N_p} \left(\frac{z_j}{s + p_j} \right) + C_0 s + 1/R_{dc} \tag{3a}$$

$$N_p = n + 2m \tag{3b}$$

where z_j can be real or complex residues, and p_j can be the real or complex conjugate poles. The C_0 and G_0 are real constants, s is the complex angular frequency and ω is the angular frequency ($s = j\omega$). The N_p is the number of poles and n and m are the number of RL and RLCG branches of the equivalent circuit fitted by VF, as shown in Fig.3. The formulae to compute each electric parameter can be found in (Vargas et al., 2005). Once the equivalent circuit of the vertical electrode is obtained, this circuit is incorporated in the GG circuit and the transient voltages can be computed by any EMTP-type programs.

3. LUMPED APPROACH FOR HORIZONTAL ELECTRODES

Several models have been proposed to represent horizontal electrodes based on the distributed or lumped circuit approaches and to compute the grounding impedance of these conductors (Sunde, 1949; Grcev e Popov, 2005; Yutthagowith et al., 2012; Yang et al., 2013). Considering that the lumped approach can be applied for a thin

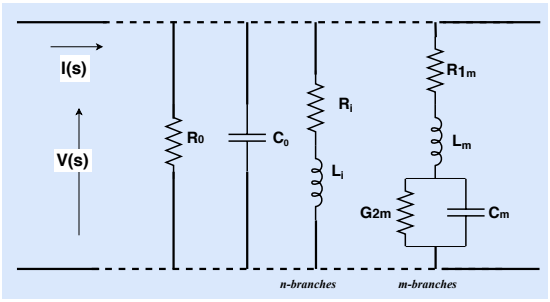

Fig. 3. Equivalent circuit for the vertical electrode admittance $Y_{eq}(s)$ fitted by VF.

uniform cylinder of radius a_h, length of l_h and burial depth of d, as shown in Fig.4.

Where μ_0, ε_0 and ρ_a are the air permeability and permittivity and resistivity, respectively. The μ_r, ε_r and ρ_s are the relative permeability, relative permittivity and resistivity of soil,respectively. Each segment of the electrode can be represented by a series resistance R_h and inductance L_h and shunt conductance G_h and capacitance C_h, as shown in Fig.4b. The horizontal conductor is divided into N segments of the same length, named elementary length, given by (Yang et al., 2013):

$$l_e = l_h/N. \tag{4}$$

If the $l_e \gg d$, the classical Sunde's equations (Sunde, 1949) can not the used. Instead, these electrical parameters can be calculated by (Cecconi et al., 2005):

$$\begin{aligned} L_h &= \frac{\mu_0 l_e}{4\pi} \left[ln\frac{2l_e}{a_h} + ln\frac{l_e}{d} - 2 + \frac{2d}{l_e} - \frac{d^2}{l_e^2} + \frac{1}{2}\frac{d^4}{l_e^4} \right]; \\ C_h &= \frac{\mu_0 \varepsilon_0 \varepsilon_r l_e^2}{2L_h}; \quad R_e = \frac{\rho_s \varepsilon_0 \varepsilon_r}{C_h}; \quad R_h = \frac{\rho_c}{\pi a_h^2} \end{aligned} \tag{5}$$

where ρ_c is the conductor resistivity and r_h is the radius of the horizontal electrode. The criterion to choose the proper size of each segment of the electrode is based on the electromagnetic radiation theory (Yang et al., 2013). For an electromagnetic wave propagating through a lossy medium, the propagation constant is given by (Cecconi et al., 2005):

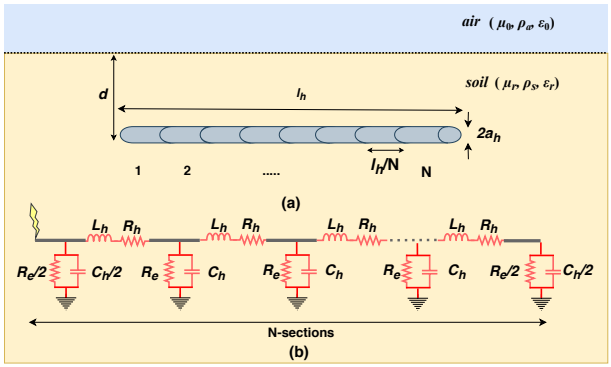

Fig. 4. Horizontal electrode buried in a given soil: [(a) HE represented by N-segments; (b) Lumped approach based on π-circuit].

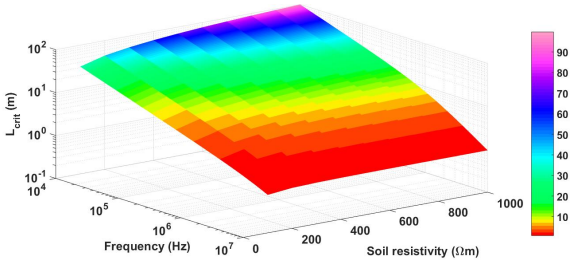

Fig. 5. Critic length (L_{crit}) as a function of frequency and soil resistivity ($\varepsilon_r = 10$; $\mu_r = 1$).

$$\gamma = \sqrt{j2\pi f\mu_m(1/\rho_m + j2\pi f\varepsilon_m)} = \alpha + j\beta, \quad (6)$$

where f is the maximum frequency of the injected current wave. The variables μ_m, ε_m e ρ_m are the relative permeability, relative permittivity and medium resistivity (soil, in this case), respectively. The term α is the attenuation constant and β is the phase constant. The wavelength is computed as follows (Yang et al., 2013):

$$\lambda = \frac{2\pi}{\beta}. \quad (7)$$

In order to respect the the "electrically small" condition, where the electrode is seen as a filamental current-carrying conductor, the maximum (critic) size (L_{crit}) of the elementary length l_e, the wavelength λ must satisfy the condition given by (Yang et al., 2013; Celli e Pilo, 2003):

$$L_{crit} = \lambda/10; \quad (8a)$$
$$2a_h/10 \ll l_e \ll L_{crit} \quad (8b)$$

Once this condition is satisfied for the maximum frequency of the injected current, each segment size l_e is seen as a carrying-conductor and the conductor can be modelled by the lumped approach (Yang et al., 2013). As an example, the critic L_{crit} is depicted in Fig.5 as a function of frequency for several soil resistivities, considering ($\mu_r = 1$, $\varepsilon_r = 10$) (Grcev e Arnautovski-Toseva, 2003). It can be noted that as the soil resistivity increases, the L_{crit} is higher, but it decreases for the increasing frequency range.

4. NUMERICAL RESULTS

4.1 Grounding Impedance of single electrodes buried in a stratified soil

The grounding impedances of the vertical electrode buried in a two-layer soil, depicted in Fig.1a, were computed in the frequency domain by a numerical (MoM) in the full-wave electromagnetic software FEKO® (FEKO, 2014). The vertical electrode has a length L_v of 12 m and a radius r of 12.5 mm and it is buried in two-layer soil where the upper and lower layer resistivities are ρ_1 =1,000 Ωm and ρ_2 = 100 Ωm, respectively. The relative permittivity adopted is $\varepsilon_r = 10$ for both layers. The equivalent resistivity ρ_{eq} is computed by Eq.(2), considering the thickness h of 1, 3 and 5 m. The computed grounding impedances by MoM and fitted curves by the VF technique are shown in Fig.6.

It can be observed that at low frequencies all grounding impedances for these configurations present a purely resistive behaviour, so-called low-frequency resistance (R_{dc}) in the literature. The grounding impedance magnitudes are practically constant up to a certain frequency, which is denominated characteristic frequency (F_C) (Salarieh et al., 2020). Above this frequency, the grounding impedances may assume either inductive or capacitive behaviour depending on the frequency range. This is due to the fact that at low frequencies, the impedance of the electrode is governed by equivalent resistance (R_{dc}) given by:

$$|Z(\omega)\,|_{\omega\to 0} = \frac{1}{G_1'h + G_2'(L_v - h)} = R_{dc}. \quad (9)$$

Considering that longitudinal resistances r_1' and r_2' in Fig.1 are neglected in comparison with the distributed conductances G_1' and G_2' which are predominant. However, at high frequencies, the leakage current at the transversal branch G_i'-C_i' dispersed into the soil assumes significant magnitudes and either inductive or capacitive behaviour predominates depending on the frequency range. As the thickness h increases, the magnitude of the grounding impedances in low frequencies also increases as it tends to homogeneous soil of 1,000 Ωm when $h \to L_v$. These grounding impedances are approximated by VF technique (red dotted-lines) as depicted in Fig.6. As observed, an excellent agreement between the impedances computed with VF and with numerical MoM are presented. Then, each impedance curve is fitted by an equivalent circuit as detailed in Fig.3.

In order to asses the impact of the first layer thickness h, the ground potential rise (GPR) is computed for two different lighting strikes injected at the top of the vertical electrode. For these computations, the lightning currents are modelled by a double-exponential impulsive current source, given by:

$$I(t) = I_0\left(e^{-at} - e^{-bt}\right) \quad (10)$$

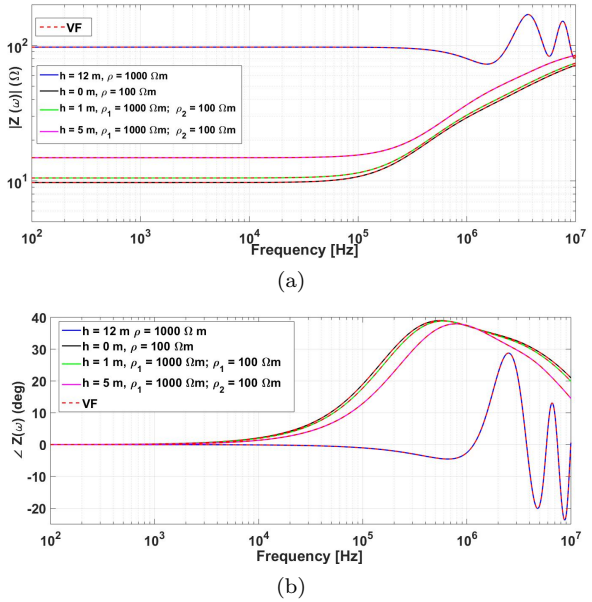

Fig. 6. Grounding impedances of the 12-m VE buried in homogeneous and two-layer soils and adjusted by the VF technique: [(a) Magnitude and (b)Phase]

where I_0 is the amplitude of the lightning current, a and b are numerical coefficients related to the rise and fall time of the function. The normalized time-domain waveforms and frequency spectra of these lightning currents are depicted in Fig.7. It can be noted that the longer current rise-time (10/350 μs) produces the shorter frequency spectra and the longer fall time correspond to a slower variation of the current in time. These characteristics are very important for the transient voltage waveforms, as further explained.

In Figs.8-9, it can be seen that for homogeneous soils, as the apparent soil resistivity increases, the GPR peaks are more significant in the transient responses. In relation to the two-layer soils, the fast-front current wave produces the highest peaks in comparison with the slow-front current. Furthermore, in the 2-layer soil, an expressive reduction is obtained due to the lower amplitude of the slow-front current, and these peaks get lower as the the thickness (h) decreases.

An horizontal electrode of length l_h = 30 m, radius a_h = 12.5 mm and buried in a homogeneous soil of ρ_s = 500 Ωm e ε_r = 10 is considered for this validation. Adopting the maximum frequency of 10 MHz, the critic

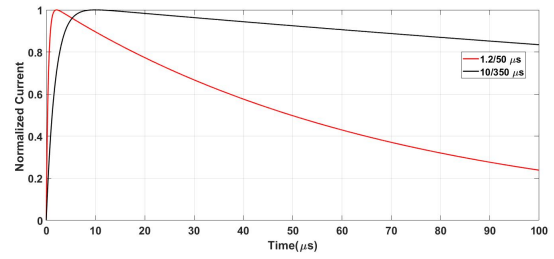

(a)

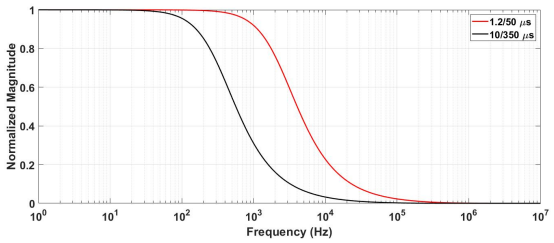

(b)

Fig. 7. Impulsive currents for the fast-front and slow-front currents: [(a) normalized time-domain waveforms and (b) normalized frequency spectra]

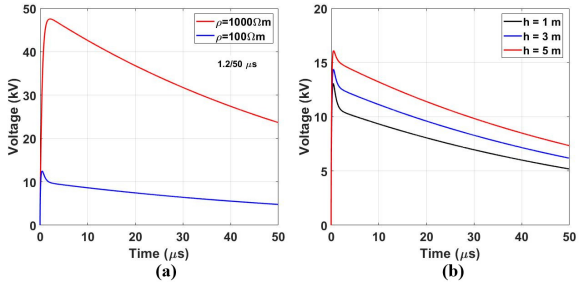

Fig. 8. GPR waveforms for the VE injected with the fast-front current: [(a) homogeneous soils and (b) two-layer soil for h = 1, 3 and 5 m].

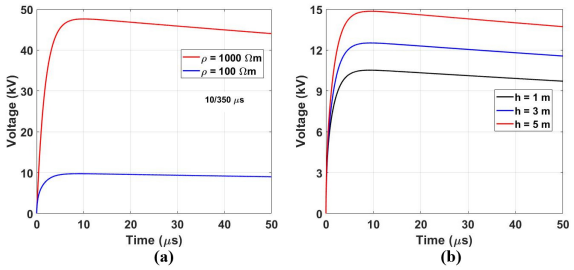

Fig. 9. GPR waveforms for the VE injected with the slow-front current: [(a) homogeneous soils and (b) two-layer soil for h = 1, 3 and 5 m].

length calculated by Eqs.(6)-(7) is L_{crit} = 1 m. This electrode is represented by N = 5, 10 and 100 π-circuits in cascade and based on Eq.(4), the elementary lengths l_e for each N are 6, 3 and 0.3 m respectively. The grounding impedances of the 30-m horizontal electrode are computed by proposed lumped approach and by TLM, using the per-unit parameters described in (Grcev e Grceva, 2009). The impedances are shown in Fig.10. It can be seen that only when N = 30 cascaded π-circuits, the condition $l_e \leq L_{crit}$ = 1 m is satisfied and the grounding impedance of the horizontal electrode computed for N = 30 presents the best agreement in relation to the grounding impedance obtained by *Transmission Line Model* as depicted in Fig.10.

Finally, a 12x12m grounding grid made of copper conductors (ρ_c = 1.72x10^{-8} Ωm), radius of 7 mm and buried at the 0.60 m is represented by the lumped approach and the node transient voltages are computed by lumped approach described in (Cecconi et al., 2005). The soil parameters are: ρ_s = 100 Ωm, ε_r = 36, μ_r = 1. The horizontal electrodes are modelled by Eqs.(5), and maximum frequency of 10

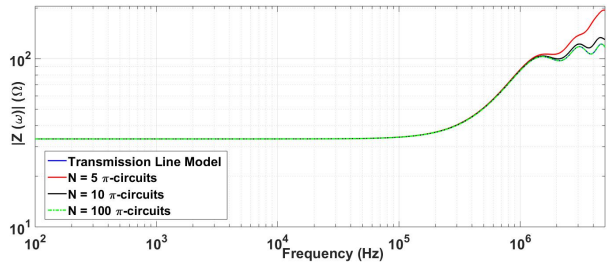

(a)

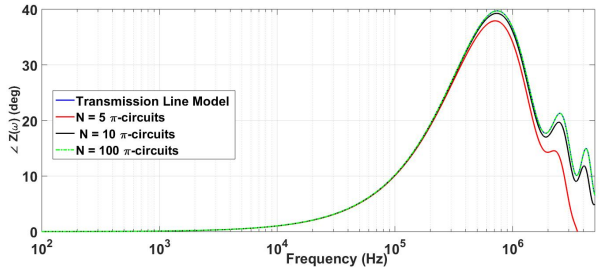

(b)

Fig. 10. Comparison of the HE grounding impedances obtained with the lumped parameter model and with transmission line model:[(a) Magnitude and (b) Phase].

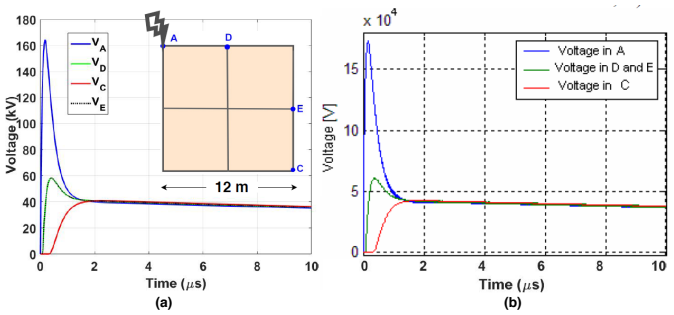

Fig. 11. Comparison of the voltages on the 12x12m GG obtained with: [(a) Proposed Approach and (b) Results from Cecconi].

MHz is considered. Using Eqs. (6) e (7), the critic length is L_{crit} = 0.483 m. The horizontal electrodes are represented by N = 50 π-circuits in cascade, the elementary length is l_e = 12/50 = 0.24 m which satisfies the condition (8). The lumped circuit is implemented in the ATP-EMTP software and the node voltages are shown in Fig.11. A double-exponential current given by i(t) = 10($e^{-143000t}$ - $e^{-5400000t}$) is injected at the upper corner. The GPR waveforms are computed in ATP-EMTP software and node voltages are depicted in Fig.11a.

In this last case, the node voltages are in accordance with the computed node voltages using the TLM as computed by (Cecconi et al., 2005).

4.2 Transient Voltages on the grounding grids

In order to compute the node voltages on a 30x30m grounding grids buried in a homogeneous and 2-layer soil, the grounding mesh composed of horizontal and vertical electrodes are represented by the lumped approach previously described. The vertical electrodes are synthesized by the VF technique and horizontal electrodes are modelled by electromagnetic radiation theory. In this study, 4 different cases are studied and they are detailed as depicted in Fig.12. The geometrical and electrical parameters for the simulations are given by:

- Horizontal : a_h = 12.5 mm, d = 0.5 m, l_h = 30 m;
- Vertical electrodes: r= 12.5 mm, L_v = 12 m;
- Homogeneous soil: ρ_1 = 1,000 Ωm; ε_r = 10; μ_r =μ_0
- 2-layer soil: ρ_1 = 1,000 Ωm; ρ_2 = 100 Ωm, ε_{r1} = ε_{r2} = 10, μ_r =μ_0;

For this analysis, the transient voltages on the GG are computed for two lightning currents which are injected at the point A of these meshes. The lightning current parameters are described in Table 1. Based on the Eqs (6) and (7) and on the condition (8), the critic length (L_{crit}) for the case 1-composed by a homogeneous soil of 1,000 Ωm, and for the stratified soils, in cases 2, 3 and 4, are shown in Table 2. For these last cases, the equivalent resistivities ρ_{eq} are calculated based on the Endrenyis's abacus which depends on the first layer thickness h (Caetano et al., 2018). For all cases, the horizontal electrode is represented by N = 30 π-circuits, which results in the elementary lengths (l_e) of 1 m, and that value satisfies condition (8). The node voltages caused by the lightning currents in points A, B, C and D are computed. The frequency-dependence on the electrical soil

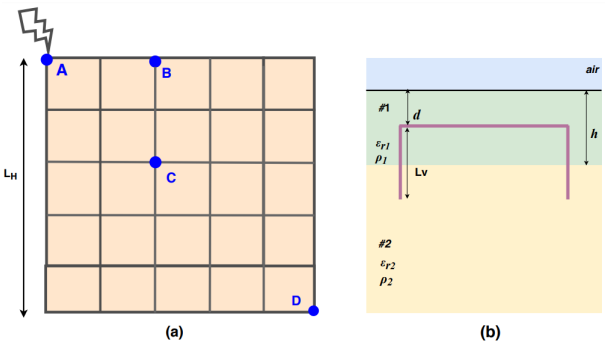

Fig. 12. Grounding grid studied: [(a) Upper view and (b) Side view].

Table 1. Lightning current parameters.

	fast-front (1.20/50 μs)	slow-front (10/350 μs)
I_0(kA)	1.037	1.025
α (s^{-1})	1.471×10^4	$2.05\ 1 \times 10^3$
β (s^{-1})	2.471×10^6	5.641×10^5

Table 2. Studied cases.

	h(m)	ρ_{eq} (Ωm)	L_{crit}(m)	l_e(m)
case 1	-	1,000	7.67	1
case 2	5	700	6.92	1
case 3	3	650	6.75	1
case 4	1	400	5.66	1

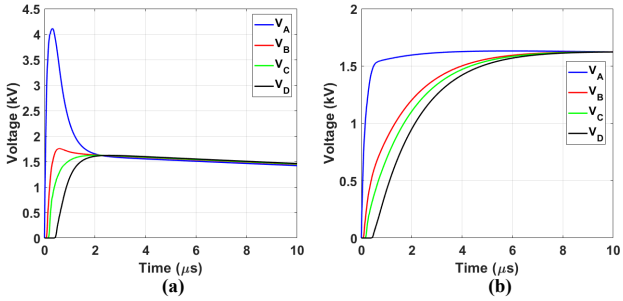

Fig. 13. Node Voltages for the grounding grid buried in a ρ_{eq}=1,000 Ωm: [(a) Fast-front wave and (b) Slow-front wave].

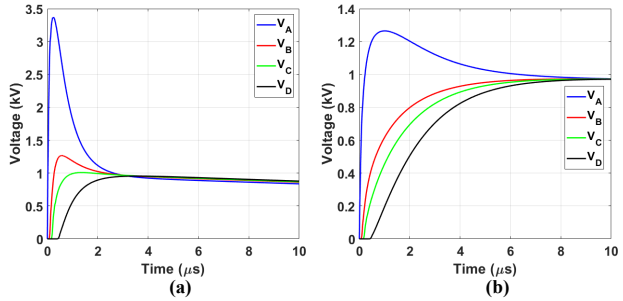

Fig. 14. Node Voltages for the grounding grid buried in a ρ_{eq}=700 Ωm: [(a) Fast-front wave and (b) Slow-front wave].

parameters, ionisation and mutual effects are not taken into account in these simulations. The simulated transient voltages for the cases 1 to 4 are shown in Figs.13-16.

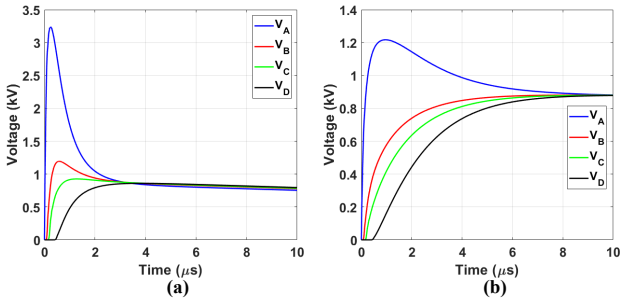

Fig. 15. Node Voltages for the grounding grid buried in a ρ_{eq}=650 Ωm: [(a) Fast-front wave and (b) Slow-front wave].

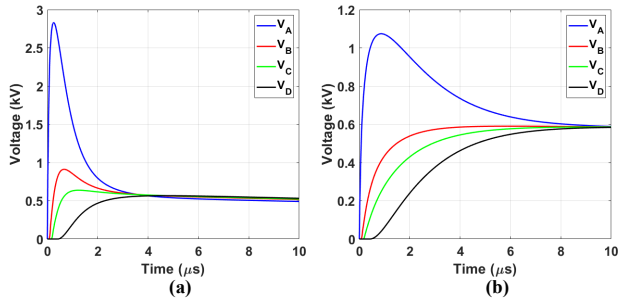

Fig. 16. Node Voltages for the grounding grid buried in a ρ_{eq}=400 Ωm: [(a) Fast-front wave and (b) Slow-front wave].

It can be seen that, independently of lightning current waveform, the highest voltage peaks are obtained at the injection point A and the lowest peaks occur at the points D, which present a delay in the transient responses. The fast-front lightning current produces the highest peaks at the injection point in each case. These peaks decreases as thickness h of the first layer decreases, due to the fact that the equivalent soil resistivity (ρ_{eq}) decreases (see Table 2). The computed voltage peaks are shown in Table 3, where it can be observed a pronounced reduction at the voltage peaks for each case. However, for the slow-front lightning wave, the transient voltage peaks are lower with a longer delay to reach 1 kV in comparison with the transient produced by the fast-wave transients, as depicted in Table 4. The percentage error, $\epsilon(\%)$, for all transient voltage peaks as the thickness h changes, in comparison with the case 1, is calculated by:

$$\epsilon(\%) = \frac{\left\| V_j^{case1} - V_j^{case(i)} \right\|}{V_j^{case1}} * 100\%; \qquad (11)$$

where j = A, B, C, D and i = 2, 3, 4. The errorss are presented in Table 5 and 6 for the fast and slow-front lightning currents, respectively.

It can be noted that the as the thickness decreases, the deviation is more significant, especially for the point D. As advantages of the proposed approach, new arrangements and grounding grids of complex topology can be analysed by this equivalent circuit which can be inserted in any EMTP software and they can analysed directly in time domain without the frequency domain analysis or inverse Laplace transforms.

Table 3. Voltage peaks (kV) in nodes A, B, C, D for a fast-front wave (1,20/50 μs).

	Voltage Peaks (kV)			
Node	Case 1	Case 2	Case 3	Case 4
A	4.112	3.373	3.240	2.833
B	1.756	1.266	1.195	0.912
C	1.622	1.009	0.927	0.638
D	1.620	0.955	0.860	0.567

Table 4. Voltage peaks (kV) in nodes A, B, C, D for a slow-front wave (10/350 μs).

	Voltage Peaks (kV)			
Node	Case 1	Case 2	Case 3	Case 4
A	1.631	1.265	1.217	1.074
B	1.622	0.973	0.880	0.590
C	1.622	0.972	0.879	0.586
D	1.622	0.971	0.878	0.584

Table 5. Errors for the transient voltages for a fast-front wave (1,20/50 μs).

Node	Case 2	Case 3	Case 4
A	18.0%	21.2%	31.1%
B	27.9%	32.0%	48.1%
C	37.8%	42.9%	60.7%
D	41.1%	46.9%	65.0%

Table 6. Errors for the transient voltages for a slow-front wave (10/350 μs)

Node	Case 2	Case 3	Case 4
A	22.4%	25.4%	34.2%
B	40.0%	45.7%	63.6%
C	40.1%	45.8%	63.9%
D	40.1%	45.8%	64.0%

5. CONCLUSIONS

This paper has presented a lumped approach to represent grounding grids with vertical electrodes buried in stratified soils under lightning currents. The vertical electrodes buried in a stratified soil are represented by equivalent circuit obtained from the Vector Fitting, which has shown an excellent agreement. The horizontal electrodes are modelled by the lumped approach which the elementary length must satisfy the condition (8) under the maximum frequency of the injected current into the conductor. For vertical electrodes, results show that as the thickness of the first layer of soil increases, the voltage peaks of the GPR waveforms also increases. The GPR peaks produce by fast-front current waves are slightly higher than the ones obtained for slow-front waves, due to higher frequency content of the first type of current wave. Impedance of horizontal electrode have shown a good agreement in comparison with the Transmission Line Model, for the proper elementary length selected.

Finally, for grounding grids in stratified soils, the transient voltages are affected by the thickness of first layer of the soil as well as by the type of the current injected in the mesh. The highest peaks are produced for the fast-front wave current in the homogeneous soil. As the thickness of the first layer increases, the equivalent resistivity increases and so thus the voltage peaks. The variation in the

voltage peaks are more pronounced at the opposite corner due to higher delay of the propagation of the surge voltage waves on the mesh combined with the lower soil resistivity for the lower thickness of the first layer (case 4). The proposed lumped representation is a friendly tool to compute grounding impedances and transient voltages on grounding grids with cylindrical rods in stratified soils combined with low computational time.

ACKNOWLEDGEMENTS

This study received Financial support from São Paulo Research Foundation (FAPESP) (Grant: 2019/01396-1) and the Management Center of Technology and Innovation (CGTI).

REFERENCES

Baba, Y., Nagaoka, N., e Ametani, A. (2005). Modeling of thin wires in a lossy medium for FDTD simulations. *IEEE Transactions on Electromagnetic Compatibility*, 47(1), 54–60. doi:10.1109/TEMC.2004.842115.

Batista, R. e Paulino, J.O.S. (2019). A practical approach to estimate grounding impedance of a vertical rod in a two-layer soil. *Electric Power Systems Research*, 177, 105973.

Caetano, C., Batista, R., Paulino, J., Boaventura, W., Lopes, I., e Cardoso, E. (2018). A simplified method for calculating the impedance of vertical grounding electrodes buried in a horizontally stratified multilayer ground. In *2018 34th International Conference on Lightning Protection (ICLP)*, 1–7. IEEE.

Cecconi, V., Matranga, A., e Ragusa, A. (2005). New circuital models of grounding systems and pds for emi analysis during a lightning strike. In *31st Annual Conference of IEEE Industrial Electronics Society, 2005. IECON 2005.*, 6 pp.–.

Celli, G. e Pilo, F. (2003). A distributed parameter model for grounding systems in the pscad/emtdc environment. In *2003 IEEE Power Engineering Society General Meeting (IEEE Cat. No. 03CH37491)*, volume 3, 1650–1655. IEEE.

Chiheb, S., Kherif, O., Teguar, M., Mekhaldi, A., e Harid, N. (2018). Transient behaviour of grounding electrodes in uniform and in vertically stratified soil using state space representation. *IET Science, Measurement & Technology*, 12(4), 427–435.

Colominas, I., Gómez-Calviño, J., Navarrina, F., e Casteleiro, M. (2002). A general numerical model for grounding analysis in layered soils. *Advances in Engineering Software*, 33(7-10), 641–649.

FEKO, E. (2014). Software & systems-sa (pty) ltd. *Stellenbosch, South Africa*, 7600.

Ghania, S.M. (2019). Grounding systems under lightning surges with soil ionization for high voltage substations by using two layer capacitors (tlc) model. *Electric Power Systems Research*, 174, 105871.

Ghomi, M., Mohammadi, H.R., Bak, C.L., da Silva, F.M.F., Khazraj, H., et al. (2019). Full-wave modeling of grounding system: Evaluation the effects of multi-layer soil and length of electrode on ground potential rise.

Gouda, O.E., El-Saied, T., Salem, W.A., e Khater, A.M. (2019). Evaluations of the apparent soil resistivity and the reflection factor effects on the grounding grid performance in three-layer soils. *IET Science, Measurement & Technology*, 13(4), 572–581.

Grcev, L. e Arnautovski-Toseva, V. (2003). Grounding systems modeling for high frequencies and transients: some fundamental considerations. In *2003 IEEE Bologna Power Tech Conference Proceedings,*, volume 3, 7 pp. Vol.3–.

Grcev, L. e Grceva, S. (2009). On HF circuit models of horizontal grounding electrodes. *IEEE Transactions on Electromagnetic Compatibility*, 51(3), 873–875.

Grcev, L. e Popov, M. (2005). On high-frequency circuit equivalents of a vertical ground rod. *IEEE Transactions on power delivery*, 20(2), 1598–1603.

Gustavsen, B. e Semlyen, A. (1999). Rational approximation of frequency domain responses by vector fitting. *IEEE Transactions on Power Delivery*, 14(3), 1052–1061. doi:10.1109/61.772353.

Kherif, O., Chiheb, S., Teguar, M., Mekhaldi, A., e Harid, N. (2017). Time-domain modeling of grounding systems' impulse response incorporating nonlinear and frequency-dependent aspects. *IEEE Transactions on Electromagnetic Compatibility*, 60(4), 907–916.

Liu, Y., Theethayi, N., e Thottappillil, R. (2005). An engineering model for transient analysis of grounding system under lightning strikes: Nonuniform transmission-line approach. *IEEE Transactions on Power Delivery*, 20(2), 722–730.

Salarieh, B., De Silva, J., e Kordi, B. (2020). On the high frequency response of grounding electrodes: Effect of soil dielectric constant. *IET Generation, Transmission & Distribution*.

Sarajcev, P. e Vujevic, S. (2009). A review of methods for grounding grid analysis. In *SoftCOM 2009-17th International Conference on Software, Telecommunications & Computer Networks*, 42–49. IEEE.

Sekki, D., Nekhoul, B., Kerroum, K., Drissi, K.E.K., e Poljak, D. (2014). Transient behaviour of grounding system in a two-layer soil using the transmission line theory. *automatika*, 55(3), 306–316.

Sunde, E.D. (1949). *Earth conduction effects in transmission systems*. Dover Publications Inc.

Vanegas, A., Velilla, E., Acevedo, W., Valencia Velasquez, J., e Moreno, G. (2008). Using a grounding system equivalent circuit to evaluate transferred lightning surges trough distribution transformers. *2008 IEEE/PES Transmission and Distribution Conference and Exposition: Latin America, T and D-LA*. doi:10.1109/TDC-LA.2008.4641788.

Vargas, M., Rondon, D., Herrera, J., Montana, J., Jimenez, D., Camargo, M., Torres, H., e Duarte, O. (2005). Grounding system modeling in emtp/atp based on its frequency response. In *2005 IEEE Russia Power Tech*, 1–5.

Yang, L., Wu, G., e Cao, X. (2013). An optimized transmission line model of grounding electrodes under lightning currents. *Science China Technological Sciences*, 56(2), 335–341.

Yutthagowith, P., Kunakorn, A., Potivejkul, S., e Chaisiri, P. (2012). Transient equivalent circuit of a horizontal grounding electrode. In *2012 International Conference on High Voltage Engineering and Application*, 157–161. IEEE.